Journal of Thermal Science Vol.26, No.3 (2017) 208–213

DOI: 10.1007/s11630-017-0931-x **Article ID: 1003-2169(2017)03-0208-06**

Study of Unsteady Flow Simulation of Backward Impeller with Non-uniform Casing

War War Min Swe[1], Hiroya MORIMATSU[1], Hidechito HAYASHI[1], Tetsuya OKUMURA[1] and Ippei ODA[2]

1. Nagasaki University, 1-14 Bunkyo-machi, Nagasaki 852-8521, Japan
2. Panasonic Ecology Systems Co., Ltd., 4017 Aza Shimonakata takaki-cho, Kasugai, 486-8522, Japan

The flow characteristics of the centrifugal fans with different blade outlet angles are basically discussed on steady and unsteady simulations for a rectangular casing fan. The blade outlet angles of the impellers are 35° and 25° respectively. The unsteady flow behavior in the passage of the impeller 35° is quite different from that in the steady flow behavior. The large flow separation occurs in the steady flow field and unsteady flow field of the impeller 35°, the flow distribution in the circumferential direction varies remarkably and the flow separation on the blade occurs only at the back region of the fan; but the steady flow behavior in the impeller 25° is almost consistent with the unsteady flow behavior, the flow distribution of the circumferential direction doesn't vary much and the flow separation on the blade hardly occurs. When the circumferential variation of the flow in the impeller is large, the steady flow simulation is not coincident to the unsteady flow simulation.

Keywords: Centrifugal fan, Impeller, Blade outlet angles, Steady and unsteady simulation, Rectangular casing

Introduction

The turbo fan design is usually made with the steady flow simulation. Then the flow out of the impellers is connected to the casing region only at the location that the impeller is in the simulation, even though the impeller is rotating and the flow characteristics are varied with the impeller location. When the flow separation occurs in the impeller, the influence of the separation is restricted in the casing located at the impeller. But in the actual flow, the influence of separation of the impeller is spread widely to the circumferential location. In most cases, flow separation is responsible for performance deterioration and higher energy loss. Generally, the efficiency and loss calculations, however, reveal a significant discrepancy between the steady and unsteady simulation.

Flow pattern in centrifugal fans is uneven because of flow separation and recirculation zones in the flow passages. Hence, many researchers contributed to increasing the efficiency of the fan by novel approaches both numerically and experimentally. The centrifugal fan with backward-curved impeller has been studied by experiments and simulations. The flow characteristics have been researched to improve the fan performance [1], [2], [4] and the interaction between the tongue and the impeller has been investigated[3]- [5]. The performance of various geometries of the impeller and shroud are examined with experiments [6]. For the case of the air conditioner, there are studies on the interaction between the impeller and the heat exchanger [7]−[9]. As to the flow characteristics of the centrifugal fan with a rectangular casing, the performance of the fan is not influenced by the length of the rectangular casing [8].

The objectives of this paper are to investigate the influence of unsteady behavior in the impeller, the casing and the fan on performance and internal flow patterns.

Received: October 2016 Hidechito HAYASHI: Professor, Ph.D.

Nomenclature

B	number of blades	ϕ	flow coefficient
D	diameter (mm)	ψ	pressure coefficient
H	span height (mm)	η	efficiency
N	rotational speed (1/min)	ω	angular velocity (rad/s)
P	pressure (Pa)	**Subscripts**	
Q	volume flow rate (m^3/s)	1	impeller inlet
T	torque (Nm)	2	impeller outlet
t	blade thickness (mm)	c	casing
Greek letters		d	design in impeller
β	blade angle (°)	s	static
		t	total

And the cause for the above discrepancy is discussed, considering the physical aspects of the computations, steady Reynolds-averaged Navier-Stokes (RANS) and unsteady Reynolds-averaged Navier-Stokes (URANS).

Geometry of Impellers

The geometries of the impellers are shown in Fig. 1. Two types of impeller are used with different blade outlet angles and other dimensions are the same. The outlet angles 35° and 25°, are the impeller 'A' and impeller 'B' respectively. The comparison of blade outlet angles is shown in Fig. 1 (a). The inlet and outlet diameters of the impellers are 142 and 230 mm. The exit blade height is 60.5 mm. Inlet angle is 15°. Its main dimensions are shown in Table 1. The impeller is attached to a rectangular shaped casing and its size is 350 mm × 350 mm × 158.3 mm.

Simulation Conditions

The steady and unsteady calculations were done with four different flow coefficients of ϕ = 0.014, 0.121, 0.187 and 0.22, among which ϕ = 0.187 is the design flow coefficient. The turbulence model is shear stress transport (SST). The computational domain consists of three domains, namely, inlet, rotating and outlet domain. The total numbers of meshes for all domains are about 5 million with tetra mesh. The minimum size of tetra mesh is 0.8 mm. The rotating speed of the impeller is 1100 r/min. The boundary conditions are defined with the mass flow rate at the inlet and 0 Pa of static pressure at the outlet. The frame change between the impeller and casing regions is imposed by Frozen-Rotor interface in the steady calculation and Transient Rotor-Stator interface in the unsteady calculation, because the flow characteristics out of the impeller are varied in circumferential location. The time step is fixed to 0.106534msec, which is equivalent to the progress of the rotor by 1° per time step. The maximum numbers of time steps are 3072 for unsteady calculation which is corresponding to 6 revolutions. The time averaged values are estimated from the data of iteration 1024 to iteration 3072.

Table 1 Main dimensions of the impellers

Specifications		Impeller 'A'	Impeller 'B'
Inlet diameter	D_1	142 mm	
Outlet diameter	D_2	230 mm	
Number of blades	B	7	
Exit blade height	H	60.5 mm	
Blade thickness	t	1 mm	
Inlet angle	β_{1d}	15°	
Outlet angle	β_{2d}	35°	25°

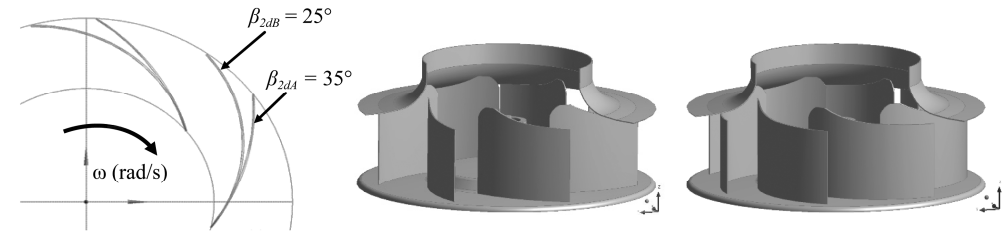

(a) Comparison of blade outlet angles (b) Impeller 'A' with β_{2dA}=35° (c) Impeller 'B' with β_{2dB}=25°

Fig. 1 Geometries of Impellers

Results and Discussions

Performance Curve

The flow rate coefficient, the static pressure coefficient, the total pressure coefficient and the efficiency in Fig. 2 and Fig. 3 are defined with the following equations.

$$\phi = \frac{60Q}{\pi^2 D^2 HN} \tag{1}$$

$$\psi = \frac{2P}{\rho\pi^2 D^2 N^2} \tag{2}$$

$$\eta = \frac{PQ}{T\omega} \tag{3}$$

Figure 2 shows the performance curves of the simulated fan. Figure 2 (a) is the static and the total pressure coefficients of fans of impeller 'A' and 'B'. For the impeller 'A', the static and total pressure coefficients in steady simulation is quite different from the unsteady simulation. But for the impeller 'B', these coefficients in steady simulation are almost the same as those in unsteady simulation. For the case of impeller 'A', the static

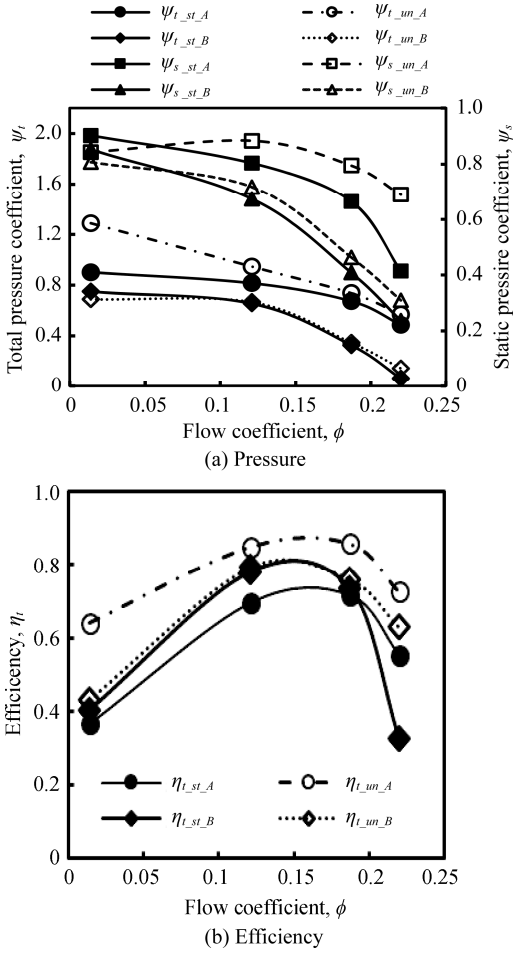

Fig. 2 Fan performance

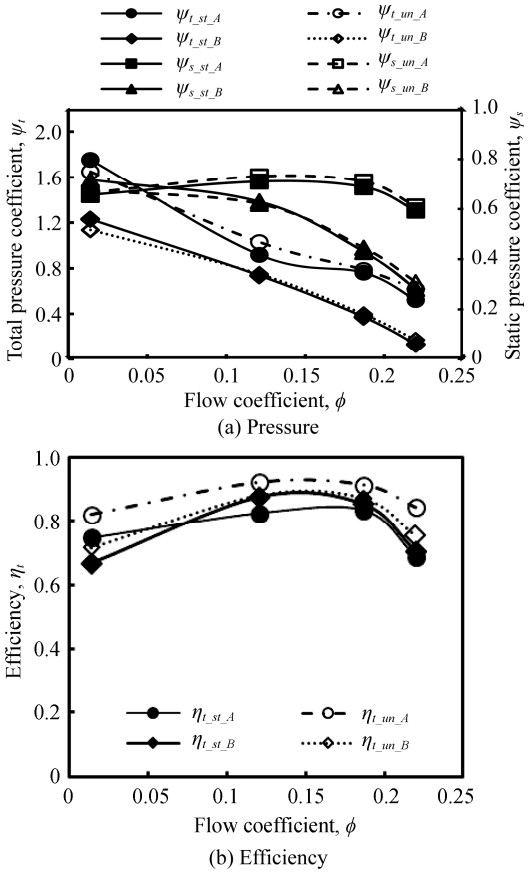

Fig. 3 Impeller performance

and total pressure coefficients are lower than in unsteady simulation. Figure 2 (b) shows the efficiency of the fans of impeller 'A' and 'B'. For the impeller 'B', the efficiency in steady simulation is well coincident to the unsteady simulation. But for the case of impeller 'A', the efficiency in steady simulation is much lower as compared with the unsteady simulation with a difference of about 0.2 in all flow rates.

The impeller performances of the impeller 'A' and 'B' are shown in Fig. 3. The steady and unsteady flow characteristics of the impeller 'A' and 'B', the static and the total pressure coefficients are shown in Fig. 3 (a) and the efficiencies in Fig. 3 (b). The performance of the static pressure and the total pressure coefficients of the impeller 'B' in steady simulation are almost the same as those in unsteady simulation. And for the case of the impeller 'A', the coefficients in steady simulation are almost the same as the case of unsteady simulation. The total pressure coefficient of the impeller 'A' is higher than that of the impeller 'B' in all flow rates, which is caused by the difference of the outlet angle of the impeller; and the variation with flow rate is similar to the impeller 'B'. But the variation of the static pressure coefficient of impeller 'A' with the flow rate is different from the case of the impeller 'B'. The static pressure of the impeller 'A' is

almost constant within a wide flow rate region but that of impeller 'B' gradually decreases with the flow rate increasing. Figure 3 (b) is the efficiency of the impeller. The efficiency of the impeller 'A' in steady simulation is lower by about 0.1 than that in unsteady simulation at all flow rates. The total pressure is almost the same in both simulations but the blade load is different in steady and unsteady simulations. The efficiency of impeller 'B' is almost the same in steady and unsteady simulations. The efficiency of the impeller 'B' in both steady and unsteady flow fields is higher than that in the steady flowfields of the impeller 'A', but those values are lower than that in the unsteady flowfields of the impeller 'A'. This shows the complexity of the impeller performance.

The casing performances, efficiency, are shown in Fig. 4. The casings have the impeller 'A' and the impeller 'B' which exhibit different casing performances under the steady and the unsteady simulations. The casing efficiency in Fig. 4 is defined by the following equation, Eq. (4).

$$\eta_c = 1 + \frac{\Delta P_{t\_C}}{\Delta P_{t\_im}} \tag{4}$$

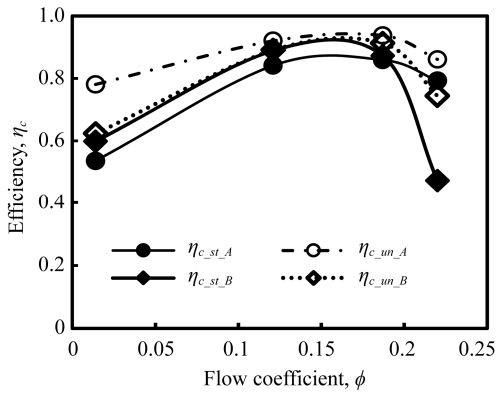

Fig. 4 Casing efficiency

The ΔP_{t_c} and ΔP_{t_im} are pressure rise in casing and the impeller, respectively. In the casing, ΔP_{t_c} is always negative. The casing efficiency based on the total pressure is the maximum at flow rate ϕ = 0.187 in all cases. The variation of the impeller 'B' is almost the same in both simulations, except for large flow rate. For the impeller 'A', the difference between the steady and unsteady simulations are large, especially at the low flow rate. The difference of the impeller 'A' at design flow rate, ϕ = 0.187, is about 0.1. The difference of the fan efficiency is about 0.2 at impeller 'A' as shown in Fig. 2 (b), which is caused by both the impeller and the casing efficiency difference.

Flow Characteristics

The flow characteristics of the simulated fans are discussed for each simulation condition at flow rate ϕ = 0.187. The flow characteristics, relative velocity and static pressure, are basically analyzed in the mid-span location of the impeller. Figure 5 shows the relative velocity contours of steady and unsteady flow patterns. The flow patterns in steady and unsteady simulations inside the impeller are quite different at impeller 'A', but for the case of impeller 'B' are almost the same. In the case of the impeller 'A' in Figs. 5 (a) and (b), the flow separation on the suction surface near the trailing edge of the blade occurs at the back region, B_2, B_3, and B_4, that causes the large wake near the lower wall of the casing and the upper corner in the steady simulation. The separation leads to a distinct wake region. But the separation is very small in unsteady simulation. And the outflow from the casing near the upper wall is large in steady simulation. The uniform flow pattern occurs in unsteady flow field inside the impeller 'A', but non-uniform flow patterns occur in the steady flow field. The steady flow pattern in the circumferential direction of casing is quite different from the unsteady flow pattern. The secondary flow is dominant in the casing and the wake occurs in the corner of the casing and fan outlet in the steady flow. In the unsteady simulation, the impeller rotates as the flow passes through the blade passage and the inlet condition and outlet condition of the impeller are varied. This operates to average the flow in the impeller. Figures 5 (c) and (d) show velocity contour of the impeller 'B' in steady and unsteady flow field. The separation occurs only at the leading edge of the suction sides of blades inside the impeller 'B'. The steady flow pattern is a little different from the unsteady flow pattern inside impeller 'B'. In both steady and unsteady cases, the flow pattern is a little different in the circumferential direction of the casing.

Figure 6 shows the pressure distributions at the design flow coefficient ϕ = 0.187. Figures 6 (a) and (b) are the cases of the impeller 'A'. The results from the steady simulation show that the flow in the impeller of Fig. 6 (a) is varied in circumferential location. The pressure at the inlet of impeller is lower than in the region of the outlet.. But the pressure is higher in the back region of the fan, B_3 to B_4. This pressure distribution continues to the impeller outlet. The static pressure is a little higher in the impeller 'A' outflow region, between B_2 and B_5 in the impeller rotational direction. In the casing, the pressure is lower at the fan exit, B_6, B_7, but higher at back region, B_3 to B_5. In the unsteady simulation, the pressure distribution in circumferential location is a little varied in the casing and is high only at the corner. The discrepancy of steady and unsteady simulation is caused by the flow from the inlet to outlet of the impeller. At the steady simulation, the impeller does not move in the entire simulation time and the flow of the impeller passage is restricted in the fixed impeller passage. Figures 6 (c) and

(d) show the case of the impeller ‘B’. The static pressure distribution in steady simulation is a little different from the unsteady one within the blade sections. The blade load of the impeller ‘B’ is lower than the impeller ‘A’, and the separation of the boundary layer on the blade surface is hardly occurs. These flow characteristics make the difference between the steady and unsteady simulation small.

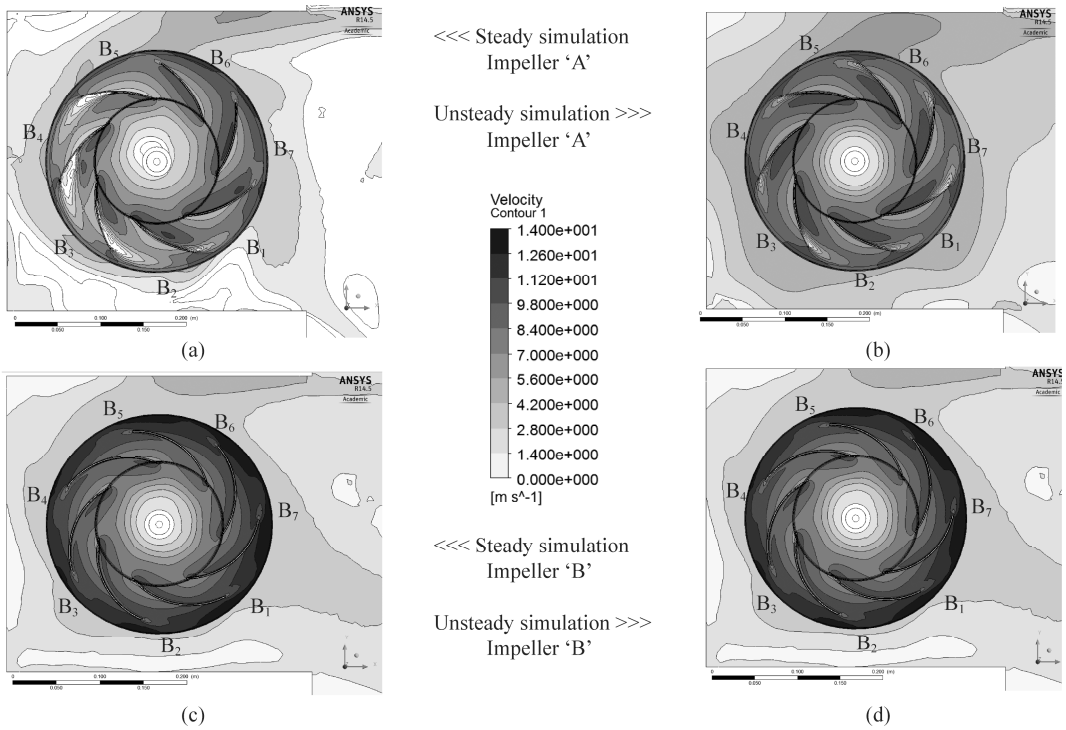

Fig. 5 Relative velocity distributions at ϕ=0.187 (mid-span section)

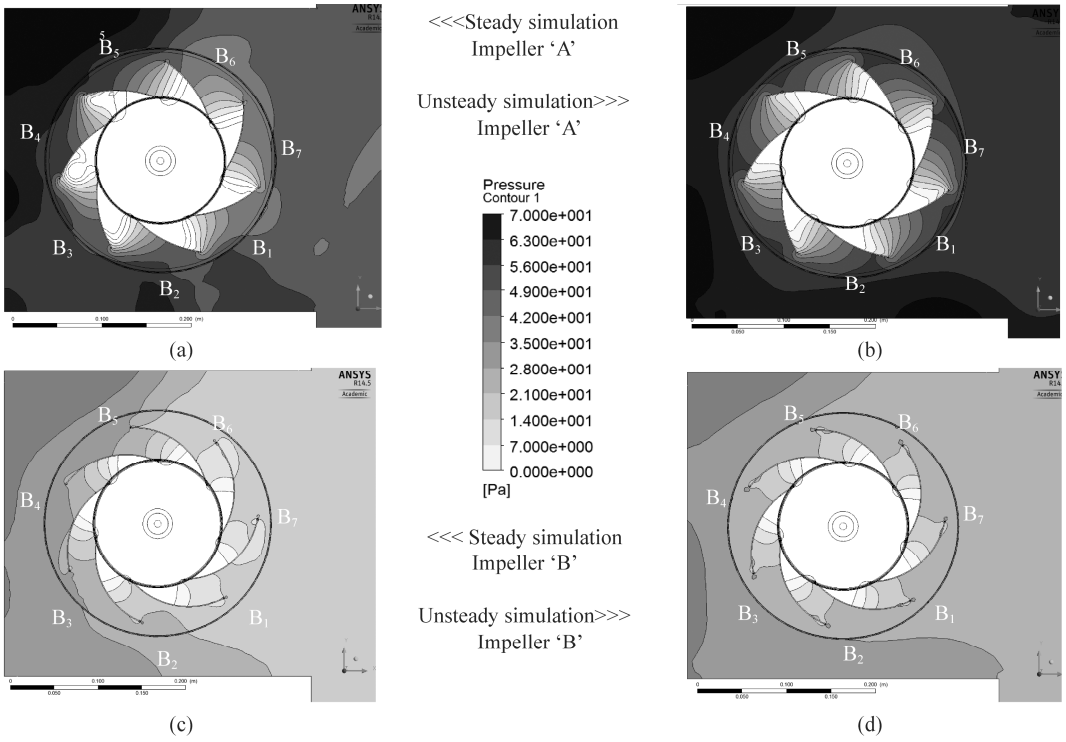

Fig. 6 Static pressure contour at ϕ=0.187 (mid-span section)

Conclusions

The effect of unsteady behavior of simulation is discussed on the performance of a centrifugal fan. Two types of blades, with small and large outlet angles, are used to research it. The following results are obtained.

1. The results of the fan performances are different in steady and unsteady simulations. The performances of the fan are lower in steady simulation.

2. The variation of the flow characteristics becomes large in steady simulation. The separation on the blade surface is large in steady simulation.

3. The differences between steady and unsteady simulations is large when the flow pattern of the impeller is varied in circumferential location.

References

[1] Yokoi, Y., Inagaki. S.: Experimental Study of Flow Feature in Spiral Casing of Turbo Fan, J. of TSJ, “Turbomachinery”, Vol.33−4, pp.241−249, (2005).

[2] Qi, D., Zhang, Y., Wen, S., and Liu, Q.: Measurement and Analysis of Three-Dimensional flow in a Centrifugal Fan Volute with Large Volute Width and Rectangular Cross Section, IMechE, Vol.220, pp.133−153, (2006).

[3] Yamazaki, Komatsu, S., Obata, T., and Yokoyama, S.: Investigation of Flow Pattern in a Backward-Curved Fan and Influence of Its Fan Shape on performance and Noise, Trans. of JSME, Vol.65−636, pp.2770−2776, (1999).

[4] Yu, Li, S., He, W., Wang, W., Huang, D., and Zhu, Z.: Numerical Simulation of Flow Field for a Whole Centrifugal Fan and Analysis of the effect of Blade Inlet Angle and Impeller Gap, HVAC & R Research, Vol.11−2, pp.263−283, (2005).

[5] Jeona, W.H., and Leeb, D.J.: A numerical study on the flow and sound fields of a centrifugal impeller located near a wedge, J. Sound, and Vibration, Vol.266, pp.785−804, (2003).

[6] Behzadmehr, A., Piaud, J.B., Oddo, R., and Mercadier, Y.: Aero-Acoustical Effects of Some Parameters of a Backward–Curved Centrifugal Fan, DOE, Vol.12-2, pp.353−365, (2006).

[7] Yamashita, S.: Silent and Super Link System of Ceiling Recessed Type Packaged Air Conditioner, Refrigeration, Vol.67, pp.622−627, (1992).

[8] Hayashi, H., Nakamura, K.: Flow Characteristics of Turbo Fan with Rectangular Casing, J. of TSJ, “Turbomachinery”, Vol. 39, No. 10, p. 624−631, (2011).

[9] Kodama, Y., Hayashi, H., Sanagi, T., and Kinoshita, K.: Noise Generated by Centrifugal Fan without Scroll Casing (Effects of the distance between the leading edge of blades and the wall of mouthpiece, the geometry at the outlet of the bellmouth and the gap of mouthpiece), Trans. of JSME, Vol. 63, pp.3025−3032, (1997).